sustainability

MDPI

Article

Preparation and Properties of High-Viscosity Modified Asphalt with a Novel Thermoplastic Rubber

Teng Wang [1,2], Zhirong Chen [1,2], Jinlong Hong [3], Zhen Liao [4], Di Wang [5,6], Dongdong Yuan [1,2], Yufei Zhang [1,2,*] and Augusto Cannone Falchetto [5,*]

1 School of Highway, Chang'an University, South 2nd Ring Road Middle Section, Xi'an 710064, China; tw@chd.edu.cn (T.W.); 2022121185@chd.edu.cn (Z.C.); ddy@chd.edu.cn (D.Y.)
2 Key Laboratory for Special Area Highway Engineering of Ministry of Education, Chang'an University, South 2nd Ring Road Middle Section, Xi'an 710064, China
3 School of Civil Engineering, Chang'an University, South 2nd Ring Road Middle Section, Xi'an 710064, China; 15572958301@163.com
4 Guangxi Communications Investment Group Corporation Ltd., Nanning 530022, China; 15777281380@163.com
5 Department of Civil Engineering, Aalto University, 02150 Espoo, Finland; di.1.wang@aalto.fi
6 Hangzhou Telujie Transportation Technology Co., Ltd., Hangzhou 311121, China
* Correspondence: zyufei@chd.edu.cn (Y.Z.); augusto.cannonefalchetto@aalto.fi (A.C.F.)

Abstract: With the increasing demand for improved road performance and sustainable development, modified asphalt is increasingly being used in pavement construction. This study investigates the preparation and properties of a novel high-viscosity modified asphalt. Firstly, different contents of novel thermoplastic rubber (NTPR) were mixed with neat asphalt to prepare high-viscosity modified asphalt (HVA). Then, the basic physical properties containing penetration, a softening point, ductility, and viscosity were conducted. Moreover, the rheological properties of the HVA before and after aging were analyzed via a dynamic shear rheometer test and a bending beam rheometer test. Finally, the dispersity of the modifier in HVA was analyzed via fluorescence microscopy. The results show that adding the NTPR restricts the flow of asphalt to a certain extent and improves the high temperature performance of asphalt. Furthermore, the apparent viscosity of HVA with various contents increases less and is always less than 3 Pa·s. Although adding NTPR makes the asphalt brittle, the HVA can meet the requirements when the NTPR is from 6% to 11%. With the increase in the NTPR, the modifier forms a mesh structure in the asphalt, enhancing its stability. Considering the above results, HVA with 10~11% of NTPR is recommended because it has better comprehensive properties.

Keywords: high-viscosity modified asphalt; basic physical properties; viscosity properties; rheological properties; fluorescence distribution

Citation: Wang, T.; Chen, Z.; Hong, J.; Liao, Z.; Wang, D.; Yuan, D.; Zhang, Y.; Falchetto, A.C. Preparation and Properties of High-Viscosity Modified Asphalt with a Novel Thermoplastic Rubber. *Sustainability* **2023**, *15*, 12190. https://doi.org/10.3390/su151612190

Academic Editor: Antonio D'Andrea

Received: 3 July 2023
Revised: 1 August 2023
Accepted: 8 August 2023
Published: 9 August 2023

1. Introduction

An asphalt binder is a crucial bonding component in asphalt mixtures, and the asphalt mastic composed of an asphalt binder and mineral powder is the primary source of the mixture's cohesion. With the rapid increase in global traffic volume and vehicle-borne load, ordinary road petroleum asphalt has high-temperature sensitivity and poor applicability to the road environment. It has been unable to meet the growing needs of traffic [1–4]. Adding modifiers such as rubber, resin, polymer, and natural asphalt to create modified asphalt can improve its performance [5–10]. Especially in harsh conditions, modified asphalt can exhibit better weather resistance than neat asphalt [11–13]. Therefore, researchers have been extensively researching the preparation and properties of modified asphalt [14–16].

According to the types of modifiers, modified asphalt can be classified into the following three categories: asphalt modified with environmentally friendly materials, asphalt modified with waste materials, and asphalt modified with high-performance materials.

Among them, asphalt modified with high-performance materials is focused on improving the performance of asphalt [17–19]. Common types of asphalt modified with high-performance materials include polyurethane-modified asphalt, polyphosphate-modified asphalt, high-modulus modified asphalt, etc. This kind of modified asphalt has been widely concerned because of its excellent pertinence and can reinforce the weak points in asphalt pavement [20–22]. Most studies have shown that styrene-butadiene-styrene copolymer (SBS)-modified asphalt has better rheological properties, and the preparation of SBS-modified asphalt was studied; the research results show that SBS-modified asphalt has better storage stability [23–26]. In addition, high-viscosity modified asphalt with excellent high-temperature rutting resistance has also attracted attention. Studies have shown that high-viscosity modified asphalt can effectively reduce the deformation and damage of asphalt pavement under high temperature conditions [27–30]. The latest research focuses on developing novel asphalt modifiers, such as carbon nanotubes, rubber crumbs, polyurethane, and so on. These novel modifiers can improve a certain aspect of the asphalt to achieve an improved performance of the asphalt [31–33]. The latest studies focus on improving the performance of asphalt pavements to meet the increasing demand for road use [34–37]. To summarize, the main research direction of asphalt modified with high-performance materials is focused on the preparation and properties of modified asphalt, and more in-depth research is especially focused on the rheological properties.

The novel thermoplastic rubber (NTPR) used in this study can enhance the adhesion between the asphalt binder and aggregate and improve the temperature sensitivity of the asphalt, making it suitable for various road structures [38–40]. Research on high-viscosity modifiers focuses on their material composition and development. Relevant studies have proven that high-viscosity modifiers can improve the high-temperature performance of asphalt [41–43]. However, as a new high-performance material, the preparation method and properties of HVA are unclear, and few studies have been conducted. The performance improvement of different NTPR contents compared with neat asphalt needs to be further investigated. This study will fill the gap in applying NTPR as a road asphalt modifier and promote the research of modified asphalt pavement.

2. Objective and Research Approach

The preparation and properties of HVA will be the focus of this study, and the following research objectives were identified:

- Prepare NTPR-modified asphalt with a content of 6% to 11% (with a 1% gap) and compare it with neat asphalt.
- Investigate the effect of the NTPR content on the basic properties and high- and low-temperature rheological properties before and after aging, and analyze the dispersion of the modifier in the asphalt.

With this objective, laboratory experiments are conducted on NTPR-modified asphalt (6–11%) and neat asphalt. Figure 1 summarizes the research methods used in this study. Firstly, different contents of the NTPR were mixed with neat asphalt to prepare the HVA. Then, a penetration test, softening point test, ductility test, and viscosity test were conducted. A dynamic shear rheometer (DSR) was used to conduct a frequency sweep test of the NTPR-modified and neat asphalts before and after aging, which obtained each asphalt's complex modulus (G^*), phase angle (δ), rutting factor, and CRRF. The bending beam rheometer (BBR) test was used to assess the low-temperature rheological properties of the asphalt and obtain the creep stiffness (S) and creep rate (m) of each asphalt. Finally, fluorescence microscopy (FM) was used to analyze the NTPR-modified and neat asphalt for modifier dispersion.

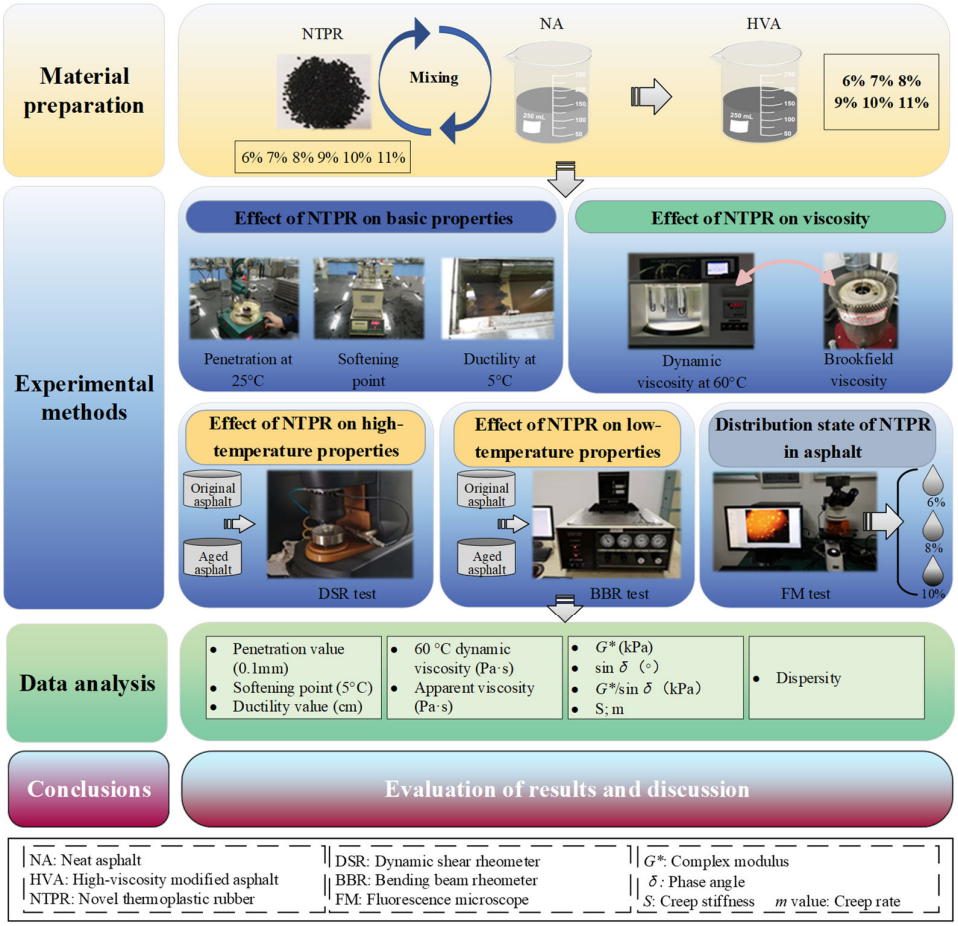

Figure 1. Research approach.

3. Materials and Methods

3.1. Raw Materials

3.1.1. Neat Asphalt

The neat asphalt used in this study was 70# road petroleum asphalt. The main performance indexes are shown in Table 1, all of which meet the relevant requirements of JTG E20-2011.

Table 1. Main technical performance indexes of neat asphalt.

Technical Index	Measured Value	Indicator Requirement	Test Basis
Penetration (25 °C, 5 s, 100 g)	72.03	60~80	T0604
Penetration index (PI)	−0.97	−1.5~+1.0	T0604
Ductility (5 cm/min, 10 °C, cm)	72.1	≥20	T0605
Softening point (°C)	47	≥46	T0606
Dynamic viscosity at 60 °C (Pa·s)	186	≥180	T0620
Density at 15 °C (g/cm^3)	1.031	/	T0603
Quality change (%)	0.09	±0.8	T0610 and T0609
Residual penetration ratio (%)	71.6	≥61	T0604
Residual ductility at 10 °C (cm)	8.3	≥6	T0605

3.1.2. NTPR Modifier

NTPR belongs to the thermoplastic rubber type material; it has a flat black, it is granular and round in shape, and the diameter is about 2–3 mm. The specific indexes are shown in Table 2.

Table 2. Physical properties of NTPR.

Item	Measured Values
Particle size (mm)	2–3
Density (g/cm^3)	0.9
Water absorption (%)	0.3

3.2. Experimental Methods

3.2.1. Preparing HVA

In this study, HVA was prepared using a high-speed shearing machine composed of a stator and rotor. Under the shearing action of the shearing machine, the particles of NTPR were finely ground and then mixed with the asphalt. The preparation process of HVA is shown in Figure 2, and the preparation procedure was as follows:

(1) Firstly, the temperature was raised to 160 °C to melt the neat asphalt. Then, NTPR particles were slowly and uniformly added, and the mixture was stirred with a glass rod for 15 min to allow for NTPR to melt and disperse preliminarily in the asphalt.
(2) Secondly, the temperature was raised to 180 °C, and the high-speed shearing machine was started with a speed control set to 5000~6000 RPM for a shearing time of 90 min.
(3) Finally, the asphalt was heated in the oven at 160 °C for about 60 min to fully dissolve the modifier and obtain the finished HVA.

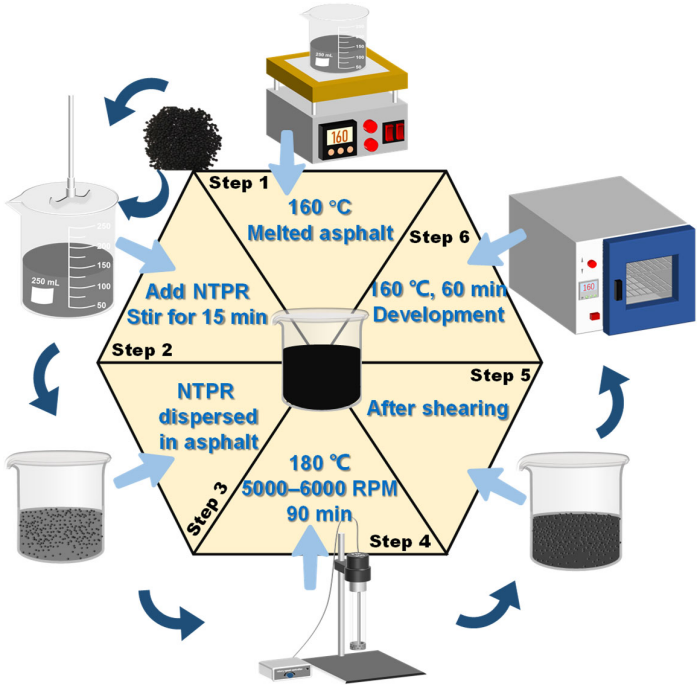

Figure 2. HVA preparation process.

3.2.2. Basic Properties Test

The HVA (6%, 7%, 8%, 9%, 10%, and 11%) was obtained according to the preparation method described in Section 3.2.1 and tested for basic property indexes. The six asphalts' basic properties were assessed via penetration at 25 °C, softening point, and ductility at 5 °C. Two specimens were tested for each binder and the average value was used as the final analysis result. Penetration was an essential indicator for evaluating the viscoelasticity of asphalt at room temperature and was of great significance for studying the rheological characteristics of asphalt. Softening point is a critical parameter for assessing the mobility of asphalt under high temperature conditions. Low-temperature ductility is closely related to pavement cracking.

3.2.3. Viscosity Test

(1) Dynamic viscosity at 60 °C

The dynamic viscosity test was conducted at 60 °C using vacuum decompression capillary and dynamic viscosity test apparatus. The test water temperature was controlled to be 60 °C, and the vacuum level was 300 ± 0.5 mmHg. The capillary tube type was selected according to whether the specimen flowed through a specific volume for more than 60 s. Seven types of asphalt were subjected to dynamic viscosity test, which were 70# neat asphalt, 6% NTPR, 7% NTPR, 8% NTPR, 9% NTPR, 10% NTPR, and 11% NTPR. Two samples of each binder were tested, and the average result is reported in this paper.

(2) Apparent viscosity test

Apparent viscosity tests were performed on 70# neat asphalt, 6% NTPR, 7% NTPR, 8% NTPR, 9% NTPR, 10% NTPR, and 11% NTPR. Each sample was tested twice, and the average value was used as the final analysis result. The instrument used was Brookfield rotary viscometer. The apparent viscosities of the above seven asphalts were determined at 60 °C, 135 °C, and 175 °C, respectively. The torque readings were controlled to be in the range of 10% to 98%. The test procedure was referred to the JTG E20-2011.

3.2.4. DSR Test

The loading often results in elastic deformation and viscous flow of asphalt. At lower temperatures, asphalt behaves as a Hookean elastic solid, while at higher temperatures, it becomes a viscous liquid, exhibiting stress relaxation with poor recovery ability [38,39]. Using DSR tests, the rheological properties of asphalt materials can be estimated, thus predicting their performance under actual road conditions. This study conducted temperature sweep tests on ten types of asphalt, which were 70# neat asphalt, HVA (6%, 7%, 8%, 9%, 10%, and 11%), and aged HVA (6%, 8%, and 10%). Two specimens were tested for each binder and the average value was used as the final analysis result. The test conditions were specified as follows: the strain was taken as 1%, the shear rate was 10 rad/s, and the test temperatures were graded according to PG as 52 °C, 58 °C, 64 °C, 70 °C, 76 °C, and 82 °C. It should be noted that the aging asphalt was tested using a rolling thin film oven test (RTFOT) to simulate the short-term aging process of asphalt. The change rate of the rutting factor (CRRF) can be used to determine the aging resistance of the asphalt binder at high temperatures. The formula used for calculating the CRRF is shown in Equation (1).

$$\text{CRRF} = \frac{\text{Aged rutting factor} - \text{Unaged rutting factor}}{\text{Unaged rutting factor}} \quad (1)$$

3.2.5. BBR Test

The principle of the BBR test is to perform a creep test of an asphalt beam specimen with dimensions of 125 mm × 12.5 mm × 6.25 mm by placing it on a support and applying a load using a hydraulic pump. A manual 3–4 g preload ensures tight contact between the beam and the support fixture. Then, a 100 g load is applied to the specimen for 1 s and held in place. The load is then released back to the preload for 20 s. After 20 s, a 100 g load is reapplied, and the test lasts for 240 s. The asphalt samples for the BBR test had seven types of asphalt, which were 70# neat asphalt, 6% NTPR, 7% NTPR, 8% NTPR, 9% NTPR, 10% NTPR, and 11% NTPR. Two specimens were tested for each binder, and the average value was used as the final analysis result. The BBR test was conducted at −12 °C and −6 °C. The S and m values at 60 s were obtained as shown in Equations (2) and (3). Besides this, the scholars proposed to use the m/S value to evaluate the low-temperature performance of asphalt, which can effectively avoid the situation that there may be contradictory situations when using S and m to evaluate the low-temperature performance of asphalt.

$$S(t) = \frac{PL^3}{4bh^3\delta(t)} \quad (2)$$

where $S(t)$ is the flexural creep stiffness at time t, MPa, P is the applied load, L is the distance, b is the width, h is the depth, and $d(t)$ is the mid-span deflection.

$$m(t) = \left| \frac{\mathrm{d}\{\lg[\mathrm{S}(t)]\}}{\mathrm{d}[\lg(t)]} \right| = |B + 2C[\lg(t)]| \quad (3)$$

where the $m(t)$ parameter is the absolute value of the slope of creep stiffness versus time, and B and C are regression coefficients.

3.2.6. FM Test

The FM can better observe the distribution of NTPR in asphalt, and a judgment can be made on the dispersion of the modifier in asphalt based on the density and uniformity of the modifier distribution [44]. Observation of 400× fluorescence is carried out using a fluorescence microscope, where the NTPR molecule can absorb energy and become activated, transitioning to an excited state when exposed to specific wavelengths of light such as blue, green, and ultraviolet light. After returning to its original state, except for the portion of energy converted into other forms, most of the energy is radiated again in the form of light energy. Therefore, the dispersion of NTPR in the asphalt can be judged based on the distribution of fluorescent spots and the strength of the light source [45,46]. The asphalt samples for the FM test had four types of asphalt, which were 70# neat asphalt, 6% NTPR, 8% NTPR, and 10% NTPR.

4. Results and Discussion

4.1. Effect of NTPR on Basic Properties

4.1.1. Effect of NTPR on Penetration

According to the test results in Figure 3, with the increase in the NTPR modifier, the penetration of the asphalt gradually decrease due to the dispersing and swelling effect that occurs during mixing, which also absorbs the lightweight components of the asphalt, forming a spatial network structure [47,48]. This spatial network structure hinders the flow of the asphalt molecules, resulting in a decrease in penetration. As the content of the NTPR increases, the spatial network structure becomes more developed, producing a more apparent inhibitory effect on the flow of the asphalt. Therefore, it leads to a more significant reduction in penetration.

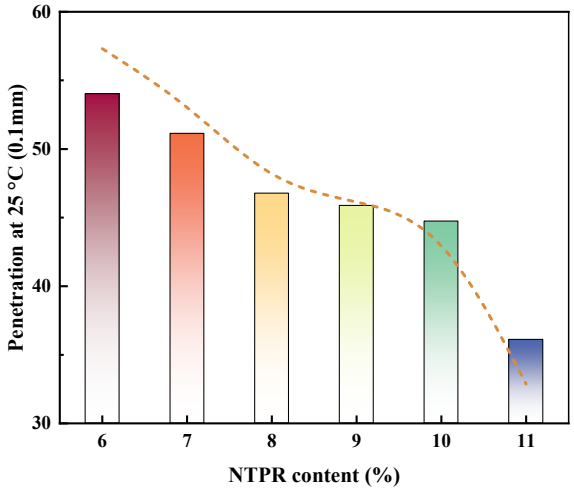

Figure 3. Variation of penetration with NTPR content.

4.1.2. Effect of NTPR on Softening Point

As shown in Figure 4, the addition of NTPR had a significant effect on the softening point of the modified asphalt, showing various degrees of improvement [49,50]. A further observation of the curve of the softening point variation with the NTPR content can be

divided into two stages. At an NTPR content below 10%, the increase in the softening point was relatively slow, indicating a relatively mild modification effect. Furthermore, when the amount of NTPR exceeded 10%, the softening point increased significantly, indicating that the modifying effect of the NTPR on the softening point of asphalt became more apparent. The effect of NTPR on the softening point is nonlinear, and the softening point increases abruptly when the NTPR dosing is more than 10%, which is likely to be caused by the formation of a mesh structure of the modifier in the asphalt.

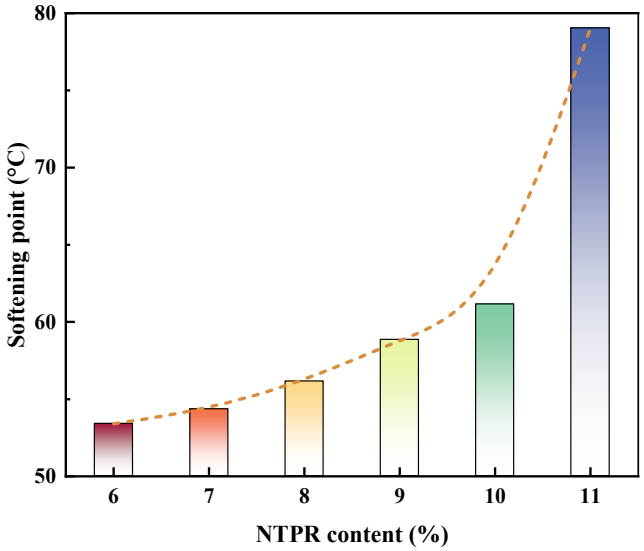

Figure 4. Variation of softening point with NTPR content.

4.1.3. Effect of NTPR on Ductility

Low-temperature ductility is an important indicator to assess the low-temperature performance of asphalt [51]. Figure 5 shows that the content of NTPR significantly affects the ductility value, which shows an increasing trend as the content of the NTPR modifier increases. However, the ductility increases and then decreases slightly when the range increases from 6% to 8%. Further, the ductility values at 5 °C and the increasing trend increases when the NTPR modifier dopes from 8% to 11%. This indicates that the modification effect gradually increases in the range of up to 11% in the NTPR content.

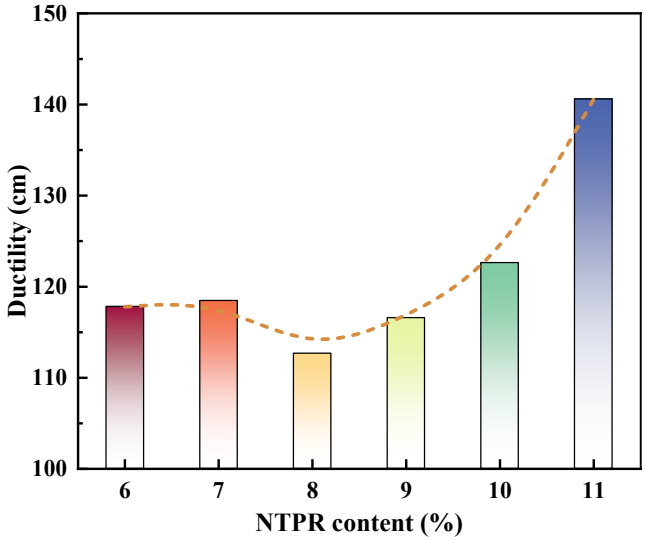

Figure 5. Variation of ductility with NTPR content.

4.2. Effect of NTPR on Viscosity

4.2.1. Effect of NTPR on Dynamic Viscosity

Based on the experimental results presented in Figure 6, it can be observed that the viscosity of modified asphalt significantly increases with the increase in the NTPR content. Within the range of 6% to 9%, the viscosity change is relatively slow, but when the content reaches 9% to 10%, the difference in the viscosity accelerates. It is worth noting that when the amount of modifier increases from 10% to 11%, the trend of the viscosity increase becomes significantly more intense. Through analysis, it can be inferred that at a lower NTPR content, the modifier cannot effectively bond various components in the asphalt structure together. It does not form a tight network structure, leading to a low and relatively uniform viscosity of the asphalt at a low content. However, when the NTPR content exceeds 10%, the NTPR can mix uniformly at various locations in the asphalt under a high-speed shearing machine, resulting in a dense mesh structure. This demonstrates that the NTPR exhibits good availability at high admixture levels and does not suffer from adhesive agglomeration. Of particular note is the higher 60 °C dynamic viscosity that facilitates the adhesion between the asphalt and aggregate when using 11% NTPR.

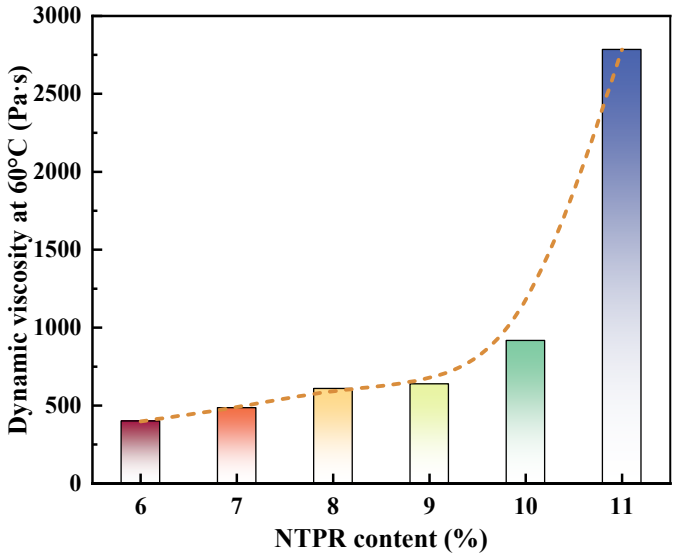

Figure 6. Variation of dynamic viscosity with NTPR content.

4.2.2. Effect of NTPR on Apparent Viscosity

The apparent viscosity test aims to control the mixing temperature of the asphalt mixture construction and to ensure the construction performance of the asphalt mixture. Figure 7 shows that the apparent viscosity of the neat asphalt is the lowest, while the HVA shows a significant increase in the apparent viscosity. Further observations of the test results at different temperatures reveal that with the increase in the modifier, the apparent viscosity value at 60 °C increased significantly. In contrast, the increase in the apparent viscosity at 135 °C and 175 °C was relatively small. This observation reveals that the combined effect of the NTPR modifier and asphalt had a more significant effect on improving the low-temperature apparent viscosity while having a more negligible impact on the high-temperature apparent viscosity. The specification recommends a temperature at 0.28 ± 0.03 Pa·s as the range for the compaction molding temperature, and recommends a temperature at a viscosity of 0.17 ± 0.02 Pa·s as the range for the mixing temperature. Based on Figure 7, we can see that the compaction temperature of the HVA is much larger than that of the neat asphalt, and the compaction temperature of 6% NTPR is 15 °C higher than that of the neat asphalt. Similarly, the mixing temperature of the HVA is also higher than the neat asphalt. Therefore, based on the consideration of the construction ease, the construction temperature of the HVA mix should be increased moderately. A

higher apparent viscosity at low temperatures helps the asphalt maintain flexibility in cold climates, effectively preventing road cracking and damage. Conversely, a lower apparent viscosity at high temperatures is very beneficial for the pumping performance of the asphalt during construction, improving the construction efficiency. Considering the ease of construction, the NTPR content can be controlled at 6% to 10%.

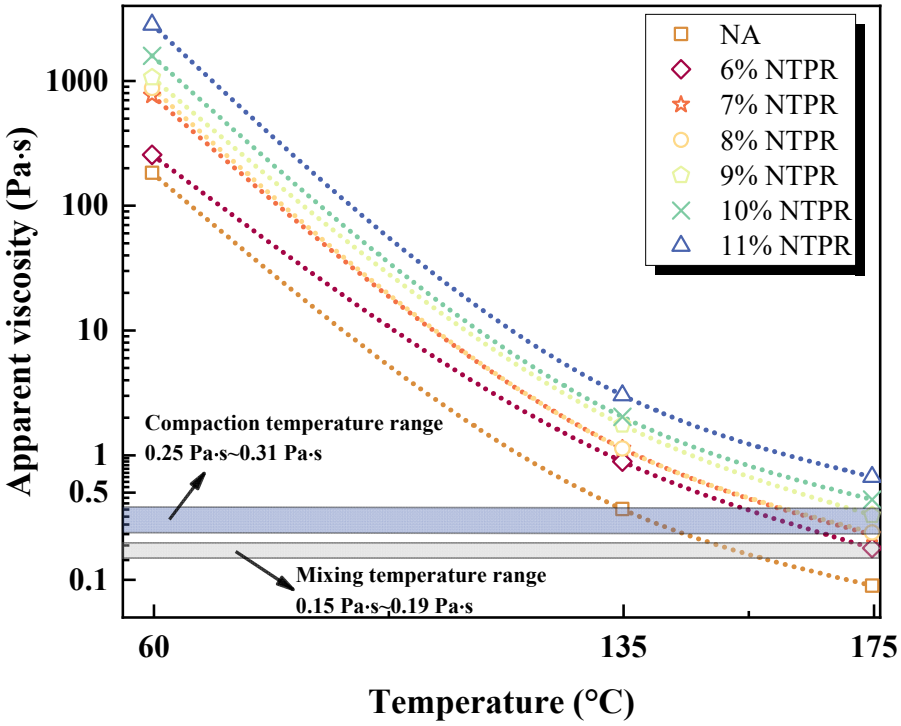

Figure 7. Apparent viscosity of HVA with different NTPR contents.

4.3. Effect of NTPR on High-Temperature Properties

4.3.1. High-Temperature Properties of HVA before Aging

A comparison of the results in Figure 8a reveals a gradual decrease in the G^* of the neat asphalt and different HVA with the increasing temperature. Specifically, the logarithmic relationship between the temperature and complex modulus shows a linear trend with the increasing temperature. This trend became more significant with an increase in the amount of the NTPR modifier. Additionally, at the same temperature, the higher the amount of NTPR modifier, the higher the complex elastic modulus of the asphalt. This result further highlights the significant impact of the NTPR modifier on the mechanical properties of the asphalt. The high content of the NTPR modifier can improve the complex elastic modulus of the asphalt, indicating that adding the modifier can enhance the elastic characteristics of the asphalt, thereby improving its resistance to deformation and mechanical stability.

The δ represents the ratio between the elastic and viscous components in the asphalt, with the value range of 0 to $\pi/2$. A smaller δ indicates that the asphalt has a more elastic component and less of a viscous component. When δ is 0, the material behaves as a Hookean elastic solid, while when δ is $\pi/2$, the material behaves as a Newtonian viscous fluid [52]. As seen in Figure 8b, the temperature has less influence on the trend of the phase angle compared to the complex modulus. Specifically, the difference in their phase angles is negligible for asphalt with 0% and 6% of NTPR modifier. Within the 7% to 10% content range, the phase angle values are relatively close and show similar trends compared to the other contents. However, when the amount of the NTPR modifier increases to 11%, the phase angle of the asphalt is the smallest, indicating that it has the best resistance to deformation under loading. This research result highlights the effect of the NTPR modifier on the phase angle of asphalt and its relationship with temperature. A lower phase angle

value indicates that the asphalt has a better elastic recovery performance and resistance to deformation under stress loading, which is crucial for the long-term stability of road structures. Through this innovative discovery, we gain a deeper understanding of the impact of the NTPR modifier on the δ and observe the difference in δ under different contents. This achievement provides essential clues for further exploring the mechanism of the NTPR modifier and optimizing its application. Future research could lead to a more precise asphalt modifier design and pavement material performance optimization based on the rheological properties of the NTPR described above [53].

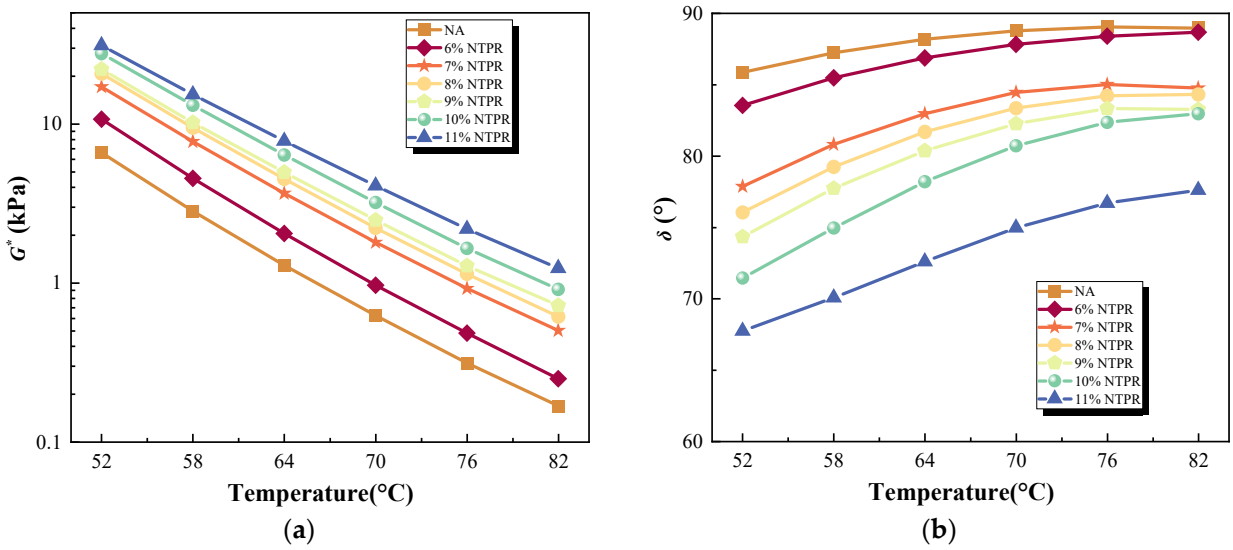

Figure 8. G^* and δ curves of HVA for each content: (**a**) G^* of HVA and (**b**) δ of HVA.

The rutting factor ($G^*/\sin\delta$) is commonly used to assess the asphalt's ability to resist permanent deformation. Generally, the larger the $G^*/\sin\delta$, the lower the flow deformation produced by the asphalt and the stronger the high-temperature performance. The study further analyzed the results in Figure 9, focusing on the $G^*/\sin\delta$ of modified asphalt with different NTPR modifier admixtures at different temperatures. The modified asphalt shows a significant decrease as the temperature increases. Specifically, the rate of change of the rutting resistance factor is faster when the temperature is increased to about 58 °C. Between 58 °C and 70 °C, the change trend gradually slows down, while above 70 °C, the change trend tends to level off. Like the complex modulus, the logarithm of $G^*/\sin\delta$ shows a linear relationship with the temperature variation. In addition, the rutting resistance factor of the modified asphalt continues to increase with the increase in the NTPR modifier admixture. Compared with the neat asphalt, the six different admixtures of the NTPR-modified asphalt show a significant advantage in the rutting resistance factor. Considering the high-temperature stability, when the NTPR content is controlled at 10~11%, the high-temperature deformation resistance of HVA is better than other dosages of HVA. This indicates that NTPR-modified asphalt has better rutting resistance and can reduce flow deformation under high temperature conditions. The results of this study highlight the effect of the NTPR modifier on the rutting resistance of modified asphalt and demonstrate the difference in rutting resistance factors at different admixtures. This provides an essential reference for further research on the optimal application of the NTPR modifier to improve the rutting resistance of road materials. Future studies can further explore the optimization of HVA by adjusting the content of the NTPR modifier to achieve a more efficient and sustainable road material design and application.

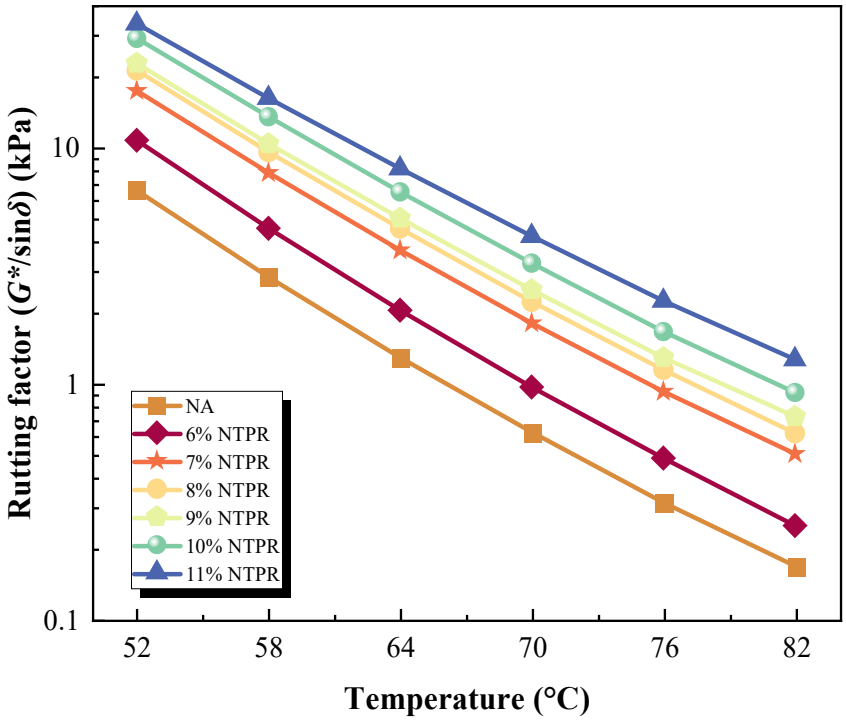

Figure 9. Rutting factor curve of HVA for each content.

4.3.2. High-Temperature Properties of HVA after RTFOT

Asphalt mixtures are subject to aging during mixing, transportation, and long-term road use, with asphalt aging during the mixing process being short-term aging [54,55]. The DSR test results of 6%, 8%, and 10% NTPR and neat asphalt after RTFOT are shown in Figure 10. From Figure 10a, it can be seen that the logarithm of the complex modulus of the aged HVA still maintains an excellent linear relationship with the temperature. As the temperature increases, the complex modulus of the aged HVA decreases subsequently. Under the same high temperature conditions, the aged HVA exhibited a higher complex modulus than the aged neat asphalt. This indicates that the HVA pavement will maintain better stability and be less prone to high-temperature deformation disease of the pavement as it passes through the service life. The complex modulus of the HVA after aging becomes more significant when the amount of the NTPR admixture increases. Figure 10b shows that the phase angle of the neat, aged asphalt approaches 90° faster when the temperature increases, and the aged HVA maintains better elastic properties under the same temperature conditions. In particular, when the temperature reaches 82 °C, the phase angle of the HVA with a 10% NTPR content is not much different from that of the neat, aged asphalt at 58 °C. This indicates that the highly doped HVA has better aging resistance than the neat asphalt.

This study further explores the effect of asphalt aging on $G^*/\sin\delta$. The results in Figure 11 show that the rutting factor of asphalt after aging increases significantly compared with that before aging. When the temperature is 82 °C, the $G^*/\sin\delta$ of the HVA after aging is higher than 1 kPa, with the latter being three times that of the neat asphalt after aging. At the same time, the phase angle of the aging asphalt also shows a decreasing trend. The modified asphalt mixed with the NTPR has a better rutting resistance than the neat asphalt after aging. This indicates that the HVA asphalt pavement will not be prone to rutting and other high-temperature diseases during the use stage. The NTPR can still play a role after high-temperature aging, making the HVA after aging maintain good high-temperature stability, which is consistent with the conclusions of previous studies [56,57].

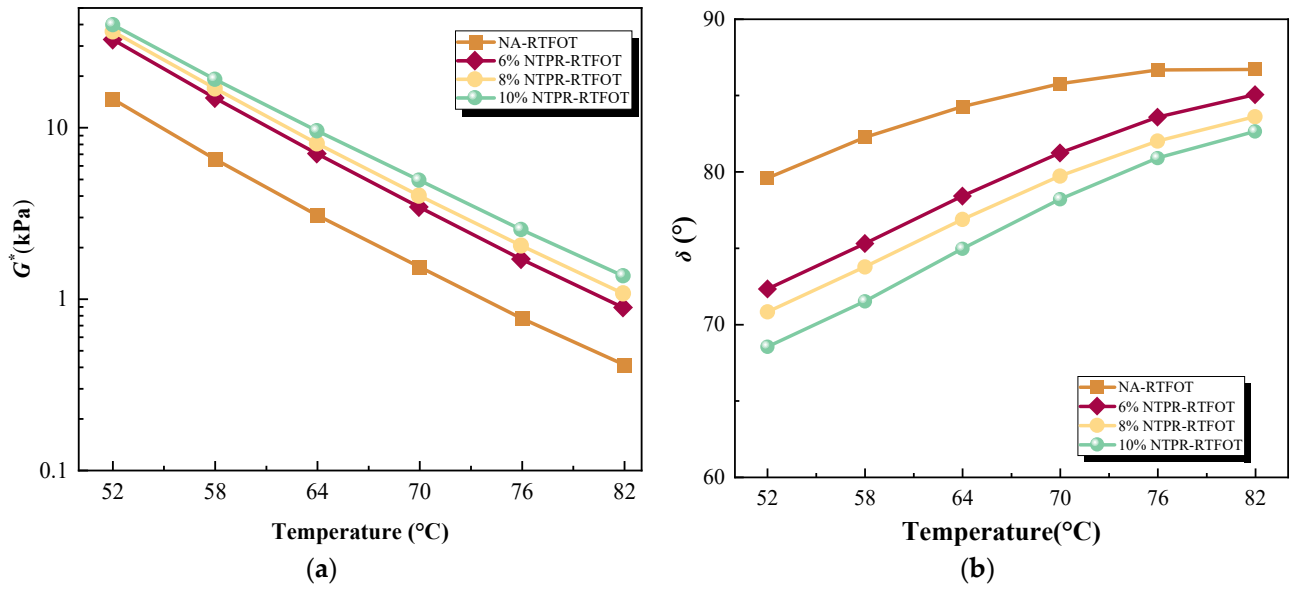

Figure 10. G^* and δ curves of HVA after aging: (**a**) G^* of HVA after aging and (**b**) δ of HVA after aging.

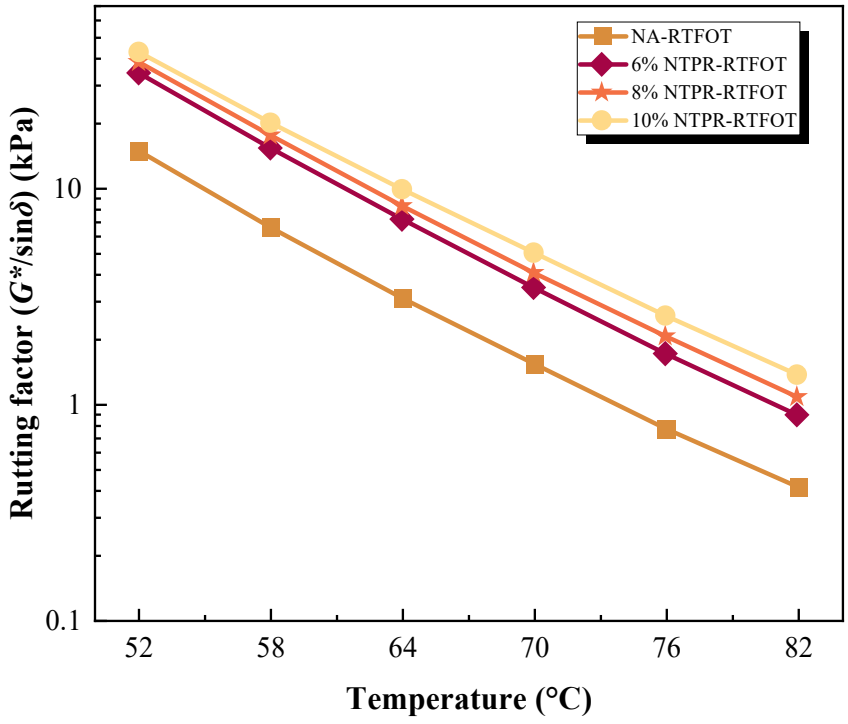

Figure 11. The rutting factor of HVA after aging.

The higher the CRRF, the worse the aging resistance of the asphalt, and the more serious the degree of aging. The CRRF has been widely used as an index to evaluate the degree of aging of asphalt. In this paper, the CRRF is used to evaluate the aging resistance of the HVA. It can be seen from Figure 12 that the CRRF of 6% NTPR is the largest in the HVA, which reaches 2.46, indicating that the aging resistance of the HVA with a low content of NTPR is poor. The anti-aging performance of 6% NTPR is not much different from that of NA. With the increase in NTPR doping, the CRRF of the HVA gradually decreases, and the aging resistance performance is enhanced. When the doping of the NTPR was 10%, the CRRF of HVA was 0.51. Compared with 6% NTPR, the aging resistance of 10% NTPR

is nearly five times higher. This indicates that the high doping of HVA has better aging resistance properties.

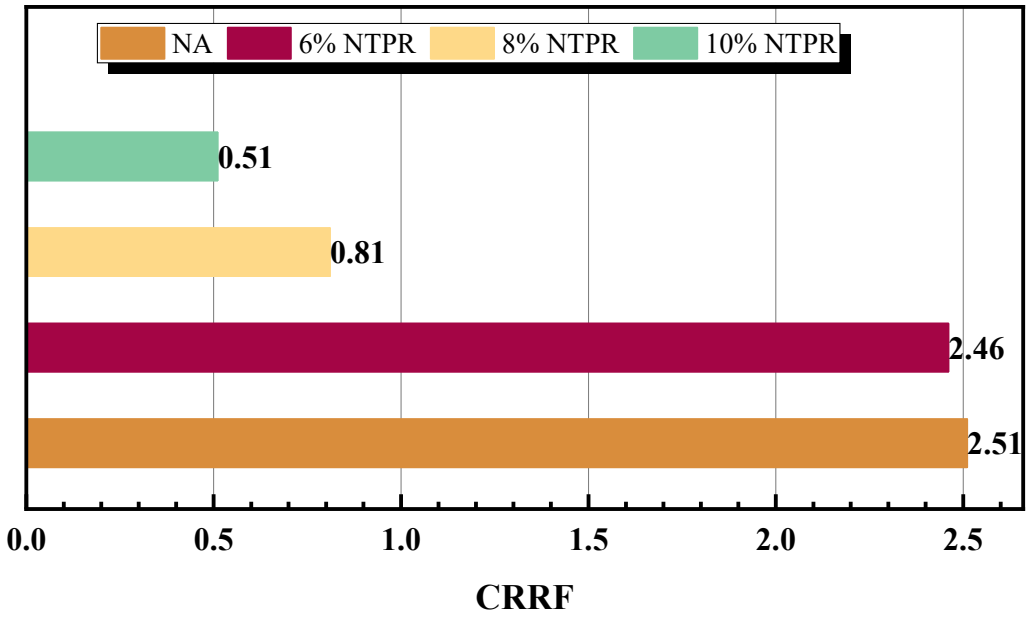

Figure 12. The rutting factor of HVA after aging.

4.4. Effect of NTPR on Low-Temperature Properties

The greater the creep stiffness obtained from the BBR test indicates that the greater the stress generated by the asphalt temperature contraction, the more brittle the asphalt, and the greater the probability of cracking [58]. The creep rate m is the rate of change of the creep stiffness S with time t. The smaller the creep rate, the slower the asphalt temperature stress relaxation, and the more likely it will crack. According to the relevant provisions of the BBR test, the stiffness of the asphalt beam should not be greater than 300 kPa, and the creep rate should not be less than 0.3. In this test, whether −6 °C or −12 °C, the neat asphalt and all NTPR-modified asphalt can meet the requirements of the corresponding specifications. Especially at −6 °C, the low-temperature properties of HVA are not much different from those of the neat asphalt. The analysis shows that adding the NTPR modifier to the neat asphalt harms the low-temperature properties of the asphalt. The modulus of the asphalt becomes larger, brittle, and easy to crack under low temperature conditions. However, it is sufficient to meet the requirements of asphalt pavement when the temperature exceeds −12 °C. On the other hand, as shown in Figures 13 and 14, the stiffness of the asphalt increases, and the creep rate decreases as the temperature decreases for all the samples, indicating a higher probability of asphalt becoming brittle and cracking under low temperature conditions. Furthermore, according to the trend of the m/S value, with an increase in the NTPR content, the m/S value remains stable, showing a slightly decreasing trend. This implies that the addition of the NTPR modifier has little impact on the low-temperature properties of the asphalt. Especially for the high-content (11%) HVA, the decrease in the m/S value is only 10% compared to the low-content (6%) HVA. Nevertheless, the low-temperature properties of 6% and 7% NTPR were slightly better than the other bitumens.

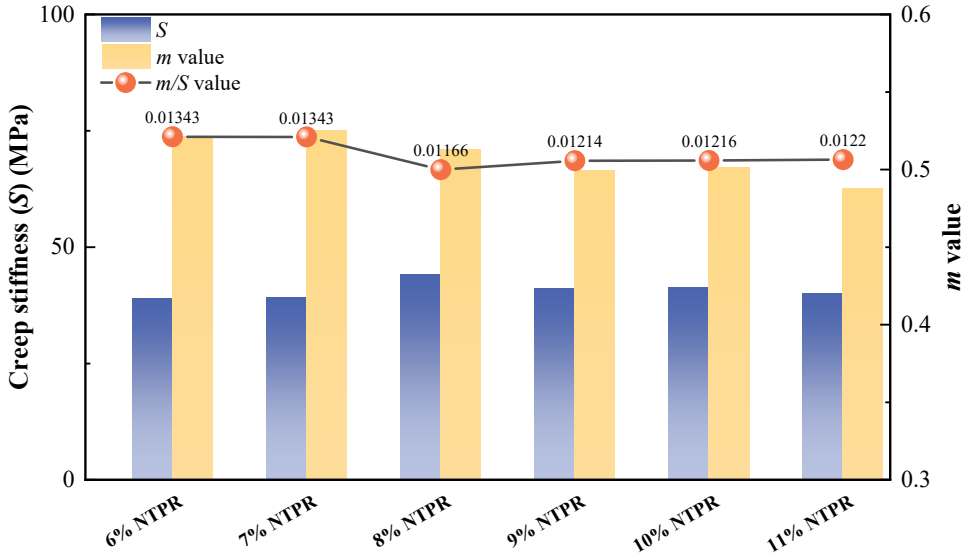

Figure 13. BBR test results at −6 °C.

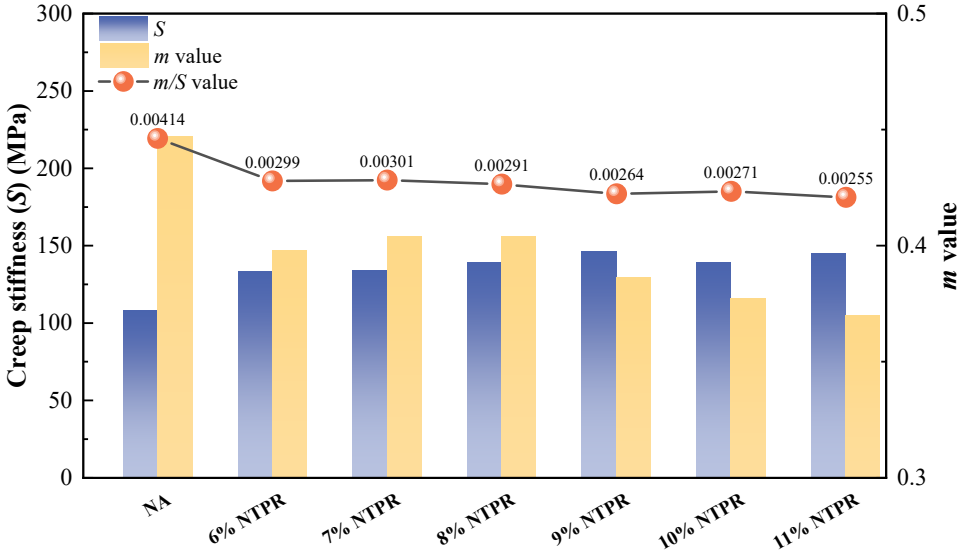

Figure 14. BBR test results at −12 °C.

4.5. Distribution State of NTPR in Asphalt

In Figure 15, the characteristic that NTPR reflects fluorescence under the irradiation of light of specific wavelengths, while the neat asphalt is dimmer under the same light irradiation, is utilized. Figure 15a shows the fluorescence image of the neat asphalt, and it can be seen that there are no fluorescent dots in the picture; Figure 15b shows the fluorescence image of 6% NTPR, and it can be seen that there are scattered fluorescent dots, namely modifier particles, in the picture. However, the NTPR did not form a network in the asphalt at this time, and was relatively independent of the asphalt. Figure 15c shows the fluorescence image of the HVA at 8%, and it can be seen that compared with the HVA at 6%, the modifier particles of the HVA at the current doping condition are more densely distributed and can be evenly dispersed in the asphalt solution; Figure 15d shows the fluorescence image of the HVA at 10%, and it can be seen that at this time, the fluorescence effect of the modifier is more intense. The particles overlap each other in contact and form a net-like structure. The properties test of the asphalt shows that when the content of the NTPR reaches 11%, the properties of the HVA show obvious differences compared with other asphalts. Combined with the fluorescence images of 10% NTPR, it can be speculated

that when the content of the NTPR is 11%, there may be a phase inversion in the asphalt, that is, the asphalt is dispersed into the modifier. This results in 11% NTPR properties that differ from other bitumens. These analyses need further experimental verification. In summary, it can be seen that as the content of the NTPR increases, the density of its distribution increases, and the fluorescence becomes more intense, and finally, at 10%, the fluorescence distribution is denser and starts to contact each other, gradually developing a mesh-like structure. The flow of neat asphalt is restricted in the structure of the NTPR, the stability is increased, and the temperature sensitivity is reduced. The 10% NTPR microstructure is quite different from the other asphalts, forming a mesh structure. This is one of the reasons why high-content HVA performs better than other asphalts.

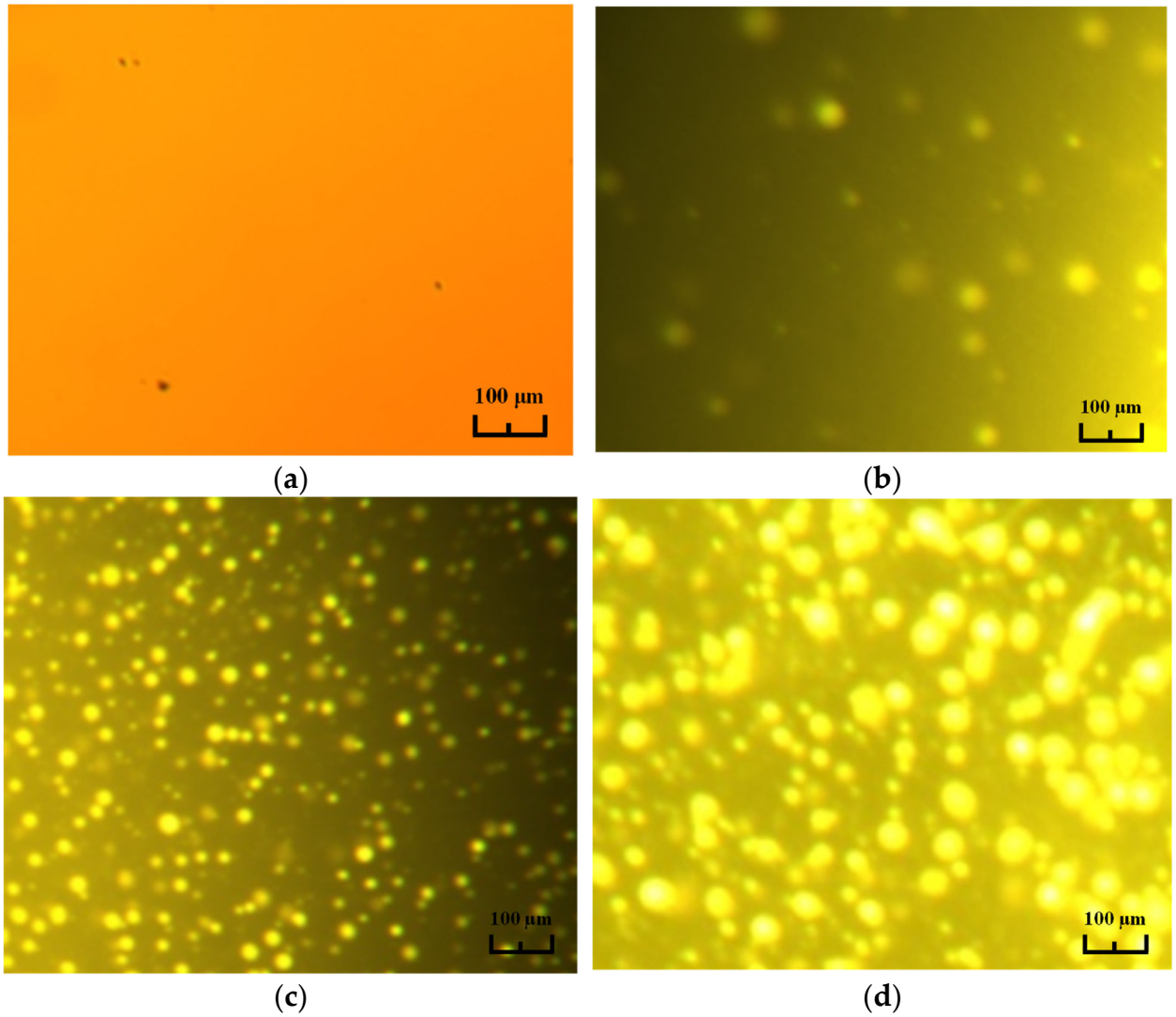

Figure 15. FM of neat asphalt, HVA (6%, 8%, and 10%): (**a**) neat asphalt; (**b**) HVA (6%); (**c**) HVA (8%); (**d**) HVA (10%).

5. Conclusions

In this study, starting from the raw materials and the modification preparation process of NTPR, six modified asphalt samples with 6~11% NTPR were prepared and compared with the neat asphalt for laboratory tests on the penetration, softening point, viscosity, high- and low-temperature rheological properties, and modifier distribution. The main conclusions are as follows:

(1) The addition of NTPR limited the flow of the asphalt to some extent and improved the high-temperature performance. This trend increased with the NTPR admixture, and the recommended NTPR admixture of 10~11% HVA has a better overall performance. Considering the economy and performance, 10% of NTPR modifier is recommended for modified asphalt preparation.
(2) The high-temperature apparent viscosity of modified asphalt increased less with the addition of NTPR. It was always less than 3 Pa·s, which is conducive to ensuring the fluidity of asphalt in construction. At the same time, the dynamic viscosity of 60 °C is more significant, which provides excellent adhesion of asphalt and aggregate.
(3) The NTPR improved the high-temperature rutting resistance of asphalt. Compared with the neat asphalt, the rutting factor of the HVA (10%) after aging at 82 °C was three times higher than that of the neat asphalt after aging.
(4) The incorporation of NTPR makes the asphalt brittle. However, when the blending amount is controlled at 6~11%, the low-temperature performance of the HVA is less attenuated, and all of them can meet the low-temperature requirements of asphalt.
(5) The density of the modifier distribution in the asphalt gradually increased and began to develop toward a mesh structure between each other with the increase in the NTPR content, which reduced the temperature sensitivity of the HVA, enhancing the stability of the HVA. When the content of the NTPR reached 10%, a mesh structure was formed inside the modified asphalt.

This study explored the preparation and properties of NTPR-modified asphalt. The basic property indexes, rheological properties, and microstructure were investigated. The contribution of the article is that the results obtained will be far reaching for the construction of modified asphalt pavements, especially for heavy traffic. It will reduce the pavement deformation diseases caused by high-temperature environments and consequently reduce road maintenance costs. However, these studies were only conducted in the laboratory, and future research should focus on field trials. In addition, a side-by-side comparison of NTPR-modified asphalt with other asphalt modified with high-performance materials should also be emphasized.

Author Contributions: Conceptualization, T.W.; methodology, T.W.; validation, Z.L.; formal analysis, Z.C.; investigation, J.H.; resources, D.W.; data curation, D.Y.; writing—original draft preparation, Y.Z.; writing—review and editing, Y.Z.; supervision, A.C.F.; project administration, Z.L.; funding acquisition, A.C.F. All authors have read and agreed to the published version of the manuscript.

Funding: This research was funded by the Guangxi Transportation Science and Technology Demonstration Project "Guilin-Zhongshan Highway Green Energy Self-consistent Supply and Efficient Utilization Key Technology Integration Application Research and Demonstration" (Grant number 2023-0002).

Institutional Review Board Statement: Not applicable.

Informed Consent Statement: Not applicable.

Data Availability Statement: Access to any other materials can be requested by writing to the corresponding authors.

Acknowledgments: The authors would like to thank the Guangxi Transportation Science and Technology Demonstration Project "Guilin-Zhongshan Highway Green Energy Self-consistent Supply and Efficient Utilization Key Technology Integration Application Research and Demonstration", grant number 2023-0002.

Conflicts of Interest: The authors declare no conflict of interest.

References

1. Ma, J.M.; Hesp, S.A.M.; Chan, S.S.N.; Li, J.Z.; Lee, S.P. Lessons learned from 60 years of pavement trials in continental climate regions of Canada. *Chem. Eng. J.* **2022**, *444*, 12. [CrossRef]
2. Chen, B.; Dong, F.; Yu, X.; Zheng, C. Evaluation of Properties and Micro-Characteristics of Waste Polyurethane/Styrene-Butadiene-Styrene Composite Modified Asphalt. *Polymers* **2021**, *13*, 2249. [CrossRef]

3. Sha, A.; Liu, Z.; Jiang, W.; Qi, L.; Hu, L.; Jiao, W.; Barbieri, D.M. Advances and development trends in eco-friendly pavements. *J. Road Eng.* **2021**, *1*, 1–42. [CrossRef]
4. Zhang, Z.; Zhang, S.; Zhao, Z.; Yan, L.; Wang, C.; Liu, H. HydroBIM—Digital design, intelligent construction, and smart operation. *J. Intell. Constr.* **2023**, *1*, 9180014. [CrossRef]
5. Yu, J.; Cong, P.; Wu, S. Laboratory investigation of the properties of asphalt modified with epoxy resin. *J. Appl. Polym. Sci.* **2009**, *113*, 3557–3563.
6. Behnood, A.; Gharehveran, M.M. Morphology, rheology, and physical properties of polymer-modified asphalt binders. *Eur. Polym. J.* **2019**, *112*, 766–791. [CrossRef]
7. Kok, B.V.; Yilmaz, M.; Turgut, P.; Kuloglu, N. Evaluation of the mechanical properties of natural asphalt-modified hot mixture. *Int. J. Mater. Res.* **2012**, *103*, 506–512. [CrossRef]
8. Ma, T.; Wang, H.; He, L.; Zhao, Y.L.; Huang, X.M. Mechanism and Performance Evaluation of Different Crumb Rubber Modified Asphalt. In Proceedings of the 1st International Conference on Transportation Infrastructure and Materials (ICTIM), Xi'an, China, 16–18 July 2016; Destech Publications, Inc.: Xi'an, China, 2016; pp. 11–19.
9. Wang, Z.; Gong, F.; Maekawa, K. Multi-scale and multi-chemo–physics lifecycle evaluation of structural concrete under environmental and mechanical impacts. *J. Intell. Constr.* **2023**, *1*, 9180003. [CrossRef]
10. Luo, T.; Li, X.; Gao, X.; Yan, C. Study on the Effect of Different Warm Mix Additive on the Road Performance of High Viscosity Asphalt Mixtures. *J. Munic. Technol.* **2023**, *41*, 77–84.
11. Wang, H.P.; Liu, X.Y.; Apostolidis, P.; Wang, D.; Leng, Z.; Lu, G.Y.; Erkens, S.; Skarpas, A. Investigating the High- and Low-Temperature Performance of Warm Crumb Rubber-Modified Bituminous Binders Using Rheological Tests. *J. Transp. Eng. Pt. B-Pavements* **2021**, *147*, 13. [CrossRef]
12. Jia, M.; Sha, A.M.; Jiang, W.; Li, X.Z.; Jiao, W.X. Developing a solid-solid phase change heat storage asphalt pavement material and its application as functional filler for cooling asphalt pavement. *Energy Build.* **2023**, *285*, 13. [CrossRef]
13. Jiang, W.; Li, P.F.; Sha, A.M.; Li, Y.P.; Yuan, D.D.; Xiao, J.J.; Xing, C.W. Research on Pavement Traffic Load State Perception Based on the Piezoelectric Effect. *IEEE Trans. Intell. Transp. Syst.* **2023**, *24*, 8264–8278. [CrossRef]
14. Yuan, D.D.; Jiang, W.; Sha, A.M.; Xiao, J.J.; Wu, W.J.; Wang, T. Technology method and functional characteristics of road thermoelectric generator system based on Seebeck effect. *Appl. Energy* **2023**, *331*, 21. [CrossRef]
15. Jiang, W.; Yuan, D.D.; Shan, J.H.; Ye, W.L.; Lu, H.H.; Sha, A.M. Experimental study of the performance of porous ultra-thin asphalt overlay. *Int. J. Pavement Eng.* **2022**, *23*, 2049–2061. [CrossRef]
16. Yang, J.H.; Zhang, Z.Q.; Fang, Y.; Shi, J.R.; Yang, X.H. Exploration for Cohesion and Adhesion Characteristics of High Viscosity-Modified Asphalt: Impacts of Composition-Associated Factors and Thermal Aging. *J. Mater. Civ. Eng.* **2022**, *34*, 21.
17. Wu, S.X.; Xu, W.Y.; Zhang, F.F.; Wu, H. Effect of Polyurethane on High- and Low-Temperature Performance of Graphene Oxide-Modified Asphalt and Analysis of the Mechanism Based on Infrared Spectrum. *Coatings* **2022**, *12*, 590. [CrossRef]
18. Li, X.Q.; Pei, J.Z.; Shen, J.J.; Li, R. Experimental Study on the High-Temperature and Low-Temperature Performance of Polyphosphoric Acid/Styrene-Butadiene-Styrene Composite-Modified Asphalt. *Adv. Mater. Sci. Eng.* **2019**, *2019*, 16. [CrossRef]
19. Xiao, F.P.; Wang, J.Y.; Yuan, J.; Liu, Z.Y.; Ma, D.H. Fatigue and Rutting Performance of Airfield SBS-Modified Binders Containing High Modulus and Antirutting Additives. *J. Mater. Civ. Eng.* **2020**, *32*, 12. [CrossRef]
20. Wang, H.P.; Zhang, H.; Liu, X.Y.; Apostolidis, P.; Erkens, S.; Skarpas, A.; Leng, Z.; Airey, G. Micromechanics-Based Viscoelasticity Predictions of Crumb Rubber Modified Bitumen Considering Polymer Network Effects. *Transp. Res. Rec.* **2022**, *2676*, 73–88. [CrossRef]
21. Zhang, H.L.; Chen, Z.H.; Xu, G.Q.; Shi, C.J. Evaluation of aging behaviors of asphalt binders through different rheological indices. *Fuel* **2018**, *221*, 78–88. [CrossRef]
22. Zhang, H.L.; Duan, H.H.; Zhu, C.Z.; Chen, Z.H.; Luo, H. Mini-Review on the Application of Nanomaterials in Improving Anti-Aging Properties of Asphalt. *Energy Fuels* **2021**, *35*, 11017–11036. [CrossRef]
23. Sun, L.; Wang, Y.; Zhang, Y. Aging mechanism and effective recycling ratio of SBS modified asphalt. *Constr. Build. Mater.* **2014**, *70*, 26–35.
24. Sha, A.; Jiang, W.; Shan, J.; Wu, W.; Li, Y.; Zhang, S. Pavement structure and materials design for sea-crossing bridges and tunnel: Case study of the Hong Kong–Zhuhai–Macau Bridge. *J. Road Eng.* **2022**, *2*, 99–113.
25. Cuciniello, G.; Leandri, P.; Polacco, G.; Airey, G.; Losa, M. Applicability of time-temperature superposition for laboratory-aged neat and SBS-modified bitumens. *Constr. Build. Mater.* **2020**, *263*, 12.
26. Mazzoni, G.; Virgili, A.; Canestrari, F. Influence of different fillers and SBS modified bituminous blends on fatigue, self-healing and thixotropic performance of mastics. *Road Mater. Pavement Des.* **2017**, *20*, 656–670.
27. Zhou, Z.G.; Chen, G.H. Preparation, Performance, and modification mechanism of high viscosity modified asphalt. *Constr. Build. Mater.* **2021**, *310*, 9. [CrossRef]
28. Zhang, Z.P.; Chen, L.Q.; Peng, J.; Sun, J.; Zhang, D.L.; Li, X.; Wen, F.S.; Liu, H. Preparation and properties of a novel high-viscosity modified bitumen. *Constr. Build. Mater.* **2022**, *344*, 11. [CrossRef]
29. Cai, J.; Song, C.; Zhou, B.; Tian, Y.; Li, R.; Zhang, J.; Pei, J. Investigation on high-viscosity asphalt binder for permeable asphalt concrete with waste materials. *J. Clean. Prod.* **2019**, *228*, 40–51. [CrossRef]
30. Meng, X.; Zhu, J.; Shi, L.; Guo, L. Analysis and Thoughts of the Test Process of High Viscoelastic Modified Asphalt. *J. Munic. Technol.* **2023**, *41*, 133–137+167.

31. Goli, A.; Ziari, H.; Amini, A. Influence of Carbon Nanotubes on Performance Properties and Storage Stability of SBS Modified Asphalt Binders. *J. Mater. Civ. Eng.* **2017**, *29*, 9.
32. Chen, T.; Ma, T.; Huang, X.; Guan, Y.; Zhang, Z.; Tang, F. The performance of hot-recycling asphalt binder containing crumb rubber modified asphalt based on physiochemical and rheological measurements. *Constr. Build. Mater.* **2019**, *226*, 83–93.
33. Fathollahi, A.; Makoundou, C.; Coupe, S.J.; Sangiorgi, C. Leaching of PAHs from rubber modified asphalt pavements. *Sci. Total Environ.* **2022**, *826*, 10.
34. Xu, H.; Chen, J.; Sun, Y.; Zhu, X.; Wang, W.; Liu, J. Rheological and physico-chemical properties of warm-mix recycled asphalt mastic containing high percentage of RAP binder. *J. Clean. Prod.* **2021**, *289*, 125134.
35. Qian, J.; Sun, H.; Zhang, G.; Zhou, Z.; Wang, C. Evaluation of mechanical performance of high adhesive recycled asphalt with different old asphalt content. *J. Munic. Technol.* **2022**, *40*, 61–68.
36. Yang, J.H.; Zhang, Z.Q.; Shi, J.R.; Yang, X.H.; Fang, Y. Comparative analysis of thermal aging behavior and comprehensive performance of high viscosity asphalt (HVA) from cohesion, adhesion and rheology perspectives. *Constr. Build. Mater.* **2022**, *317*, 24.
37. Li, Q.; Zeng, X.; Wang, J.; Luo, S.; Meng, Y.; Gao, L.; Wang, X. Aging performance of high viscosity modified asphalt under complex heat-light-water coupled conditions. *Constr. Build. Mater.* **2022**, *325*, 126314.
38. Zhu, C.; Zhang, H.; Zhang, D.; Chen, Z. Influence of Base Asphalt and SBS Modifier on the Weathering Aging Behaviors of SBS Modified Asphalt. *J. Mater. Civ. Eng.* **2018**, *30*, 1943–5533.
39. Hugener, M.; Wang, D.; Falchetto, A.C.; Porot, L.; De Maeijer, P.K.; Oreskovic, M.; Sa-da-Costa, M.; Tabatabaee, H.; Bocci, E.; Kawakami, A.; et al. Recommendation of RILEM TC 264 RAP on the evaluation of asphalt recycling agents for hot mix asphalt. *Mater. Struct.* **2022**, *55*, 31. [CrossRef]
40. Buchler, S.; Falchetto, A.C.; Walther, A.; Riccardi, C.; Wang, D.; Wistuba, M.P. Wearing Course Mixtures Prepared with High Reclaimed Asphalt Pavement Content Modified by Rejuvenators. *Transp. Res. Rec.* **2018**, *2672*, 96–106.
41. Wang, H.P.; Liu, X.Y.; Zhang, H.; Apostolidis, P.; Erkens, S.; Skarpas, A. Micromechanical modelling of complex shear modulus of crumb rubber modified bitumen. *Mater. Des.* **2020**, *188*, 12.
42. Gao, Y.M.; Zhang, Y.Q.; Gu, F.; Xu, T.; Wang, H. Impact of minerals and water on bitumen-mineral adhesion and debonding behaviours using molecular dynamics simulations. *Constr. Build. Mater.* **2018**, *171*, 214–222.
43. Wang, H.P.; Liu, X.Y.; Varveri, A.; Zhang, H.Z.; Erkens, S.; Skarpas, A.; Leng, Z. Thermal aging behaviors of the waste tire rubber used in bitumen modification. *Prog. Rubber Plast. Recycl. Technol.* **2022**, *38*, 56–69.
44. Xu, P.J.; Zhu, Z.; Wang, Y.D.; Cong, P.L.; Li, D.G.; Hui, J.Z.; Ye, M. Phase structure characterization and compatibilization mechanism of epoxy asphalt modified by thermoplastic elastomer (SBS). *Constr. Build. Mater.* **2022**, *320*, 11. [CrossRef]
45. Jin, J.Z.; Miao, Y.Z.; Zhao, H.W.; Chen, J.; Qing, L.B.; Mu, R.; Chen, X.S.; Li, Z.X. Study on the Self-Healing Performance of Microcapsules and Microcapsule-Containing Asphalt. *Sustainability* **2022**, *14*, 12231.
46. Li, J.S.; Zhu, Y.Y.; Yu, J.Y. Study on Physical Properties, Rheological Properties, and Self-Healing Properties of Epoxy Resin Modified Asphalt. *Sustainability* **2023**, *15*, 6889.
47. Hofko, B.; Falchetto, A.C.; Grenfell, J.; Huber, L.; Lu, X.; Porot, L.; Poulikakos, L.D.; You, Z. Effect of short-term ageing temperature on bitumen properties. *Road Mater. Pavement Des.* **2017**, *18*, 108–117.
48. Guo, X.-x.; Zhang, C.; Cui, B.-x.; Wang, D.; Tsai, J. Analysis of Impact of Transverse Slope on Hydroplaning Risk Level. *Procedia Soc. Behav. Sci.* **2013**, *96*, 2310–2319. [CrossRef]
49. Wu, H.J.; Zhang, X.Y. The analysis of recovery asphalt performance in Recycled Asphalt Mixture. In Proceedings of the 3rd International Conference on Civil Engineering, Architecture and Building Materials (CEABM 2013), Jinan, China, 24–26 May 2013; Trans Tech Publications Ltd.: Jinan, China, 2013; p. 1598.
50. Zou, L.; Zhang, Y.; Liu, B.Y. Aging Characteristics of Asphalt Binder under Strong Ultraviolet Irradiation in Northwest China. *Sustainability* **2021**, *13*, 10753. [CrossRef]
51. Zhang, H.L.; Su, M.M.; Zhao, S.F.; Zhang, Y.P.; Zhang, Z.P. High and low temperature properties of nano-particles/polymer modified asphalt. *Constr. Build. Mater.* **2016**, *114*, 323–332.
52. Ma, J.M.; Nivitha, M.R.; Hesp, S.A.M.; Krishnan, J.M. Validation of empirical changes to asphalt specifications based on phase angle and relaxation properties using data from a northern Ontario, Canada pavement trial. *Constr. Build. Mater.* **2023**, *363*, 12.
53. Wang, D.; Baliello, A.; Poulikakos, L.; Vasconcelos, K.; Kakar, M.R.; Giancontieri, G.; Pasquini, E.; Porot, L.; Tusar, M.; Riccardi, C.; et al. Rheological properties of asphalt binder modified with waste polyethylene: An interlaboratory research from the RILEM TC WMR. *Resour. Conserv. Recycl.* **2022**, *186*, 16.
54. Sabouri, M.; Mirzaiyan, D.; Moniri, A. Effectiveness of Linear Amplitude Sweep (LAS) asphalt binder test in predicting asphalt mixtures fatigue performance. *Constr. Build. Mater.* **2018**, *171*, 281–290.
55. Liu, H.B.; Fu, L.X.; Jiao, Y.B.; Tao, J.L.; Wang, X.Q. Short-Term Aging Effect on Properties of Sustainable Pavement Asphalts Modified by Waste Rubber and Diatomite. *Sustainability* **2017**, *9*, 996.
56. Hao, G.; Wang, Y. 3D Reconstruction of Polymer Phase in Polymer-Modified Asphalt Using Confocal Fluorescence Microscopy. *J. Mater. Civ. Eng.* **2021**, *33*, 04020400.

57. Qin, X.; Zhu, S.; He, X.; Jiang, Y. High temperature properties of high viscosity asphalt based on rheological methods. *Constr. Build. Mater.* **2018**, *186*, 476–483.
58. Mannan, U.A.; Faisal, H.M.; Tarefder, R.A. Creep Stiffness Master Curve of Recycled Asphalt Pavement (RAP) Modified Asphalt Binders Based on Binder Beam Rheometer (BBR) Test Data. In Proceedings of the International Conference on Highway Pavements and Airfield Technology, Philadelphia, PA, USA, 27–30 August 2017; American Society of Civil Engineers: Philadelphia, PA, USA, 2017; pp. 246–255.